LASER PHYSICS

Spatiotemporal mode-locking in multimode fiber lasers

Logan G. Wright,[1]* Demetrios N. Christodoulides,[2] Frank W. Wise[1]

A laser is based on the electromagnetic modes of its resonator, which provides the feedback required for oscillation. Enormous progress has been made toward controlling the interactions of longitudinal modes in lasers with a single transverse mode. For example, the field of ultrafast science has been built on lasers that lock many longitudinal modes together to form ultrashort light pulses. However, coherent superposition of longitudinal and transverse modes in a laser has received little attention. We show that modal and chromatic dispersions in fiber lasers can be counteracted by strong spatial and spectral filtering. This allows locking of multiple transverse and longitudinal modes to create ultrashort pulses with a variety of spatiotemporal profiles. Multimode fiber lasers thus open new directions in studies of nonlinear wave propagation and capabilities for applications.

The modes of a laser resonator are three-dimensional (3D) functions that vary along the axis of the resonator, as well as in the two transverse dimensions (*1*) (Fig. 1). Each mode has a distinct resonant frequency (Fig. 1, B and D). In many cases of interest, the 3D modes are separable into so-called longitudinal and transverse modes. If the relative phases of the modes are not controlled, the output is an incoherent spatiotemporal field that results from random interference. The modes can interact with each other in the gain medium and other components of a laser.

The situation can be simplified greatly by restricting operation to a single transverse mode. With the exception of high average power, the best performance for virtually all laser parameters—e.g., ultranarrow emission spectra, ultrashort pulse duration, and ultralow noise—is achieved through lasing in a single transverse mode. Operation in multiple spatial modes, by contrast, leads to substantial complexity. Nonetheless, this technique is widely employed in high–average-power lasers, for applications that do not require high temporal or frequency precision or diffraction-limited focusing.

Highly refined techniques have been developed to control the longitudinal modes of a laser. The number of oscillating modes can range from as few as 1 to more than 1 million perfectly synchronized modes in a frequency comb (*2*). Considering the pronounced control of the electromagnetic field achieved in lasers with a single transverse mode, the lack of attention paid to higher-dimensional coherent lasing states is conspicuous. Early works did propose locking of transverse spatial modes, as well as transverse and longitudinal modes. Mode-locking of this kind was demonstrated with a few modes (*3*, *4*) and has since been observed with two transverse modes of a femtosecond Ti:sapphire laser (*5*).

Recent years have seen increased interest in linear and nonlinear wave propagation in multiple transverse modes, particularly in multimode (MM) optical fibers (*6*–*16*) and largely in anticipation of spatial division multiplexing (*17*) for telecommunications and as a platform for new fiber laser sources. The presence of disorder (through random linear mode coupling) also connects MM fibers to the field of random lasers and, more broadly, to the optical properties of complex media (*18*–*21*).

Here we employ principles of normal-dispersion mode-locking (*22*, *23*) in space and time—strong spectral and spatial filtering in addition to the high nonlinearity, gain, and spatiotemporal dispersion of the fiber medium—to achieve spatiotemporal mode-locking. The self-organized, mode-locked pulses take a variety of spatiotemporal shapes consisting of many transverse and longitudinal modes.

Lasing modes can interact through the optical nonlinearities of the gain, the saturable absorber, and the fiber medium itself. These effects occur on the time scale of a pulse and thus can couple temporal and spatial degrees of freedom. The slow relaxation of rare-earth gain media introduces an additional layer of temporally averaging nonlinear interactions. To realize the simplest demonstration of highly MM spatiotemporal mode-locking (STML), we began by constructing a cavity with a few-mode, Yb-doped gain fiber (10-μm diameter, supporting approximately three transverse modes) spliced to a highly MM passive graded-index (GRIN) fiber (which supports ~100 transverse modes). The use of a few-mode gain fiber provides spatial filtering and forces the laser gain to saturate with the total energy of the coupled modes (in general, a complex combination of the ~100 transverse modes). This therefore largely eliminates transverse gain interactions and isolates the key nonlinear interactions involved in passive mode-locking. GRIN fiber is used so that the modal dispersion within the cavity is relatively small and thus of similar magnitude to the chromatic (i.e., longitudinal mode) dispersion. As will be expanded on later, this is an important factor for achieving STML. Excitation of many modes of the GRIN fiber is accomplished by fusing the two fibers with varying spatial offsets. We employ nonlinear polarization rotation as an ultrafast saturable absorber. This cavity is readily modeled by a set of coupled generalized nonlinear Schrödinger equations (GNLSEs) and has the secondary benefit of allowing observation of highly MM mode-locking at relatively low laser powers. As a result, the cavity serves as a convenient experimental and theoretical test bed for MM laser dynamics. Simulations reveal a rich variety of stable spatiotemporal pulses (an example is shown in Fig. 2, A to C, and figs. S1 to S4, whereas others are shown in figs. S5 to S12). These pulses form from noise and take on a variety of different modal compositions.

The straightforward emergence of stable spatiotemporal mode-locking is surprising but can be understood through the comparable dispersion of transverse and longitudinal modes in GRIN fiber-based cavities, as well as the periodic spatial and spectral filtering we employ in the cavity. The formation and stability of these 3D mode-locked pulses is conceptually similar to 1D dissipative solitons and self-similar pulses in single-mode fiber (*22*, *23*). In these lasers, normal dispersion and nonlinear phase modulation lead to a chirped pulse whose duration and bandwidth grows through most of the cavity. Strong spectral filtering of this chirped pulse reduces the duration and bandwidth and thus allows the pulse to meet the periodic boundary condition of the laser. In the current study, this approach is applied in space-time: In the MM cavities, the combination of spatial and spectral filtering helps to establish a 3D steady-state pulse evolution with periodic boundary conditions in both space and time (figs. S3 and S4), a crucial aspect of mode-locking. Because in GRIN fiber the magnitude of transverse mode dispersion is similar to that of the chromatic dispersion, coupling between all types of modes is equally strong. Hence, mode-locking in such a 3D cavity generally involves numerous kinds of 3D modes.

Experimentally, spatial and spectral filtering are implemented through the overlap of the MM field with the gain-fiber input and a bandpass interference filter (fig. S13). With suitable adjustments of the filters and wave plates (an experimental algorithm is described in the methods), a variety of highly MM (10 to 100 transverse modes) spatiotemporal mode-locking states can be observed (Fig. 2, D to H, and figs. S14 to S16). The typical pulse energies range from 5 to 40 nJ, corresponding to routinely available pump powers and peak powers well below the threshold for end-facet damage. The clearest evidence for spatiotemporal mode-locking is the sudden transition in the spatial, spectral, and temporal properties as we increase or decrease the pump power through the mode-locking threshold. Because we have eliminated laser gain interactions in this cavity, our observations of a different beam profile when mode-locking occurs at slightly higher pump power can only be explained by a spatiotemporal mode-locking transition involving nonlinear interactions between many transverse families of

[1]School of Applied and Engineering Physics, Cornell University, Ithaca, NY 14853, USA. [2]Center for Research and Education in Optics and Lasers, College of Optics and Photonics, University of Central Florida, Orlando, FL 32816, USA.
*Corresponding author. Email: lgw32@cornell.edu

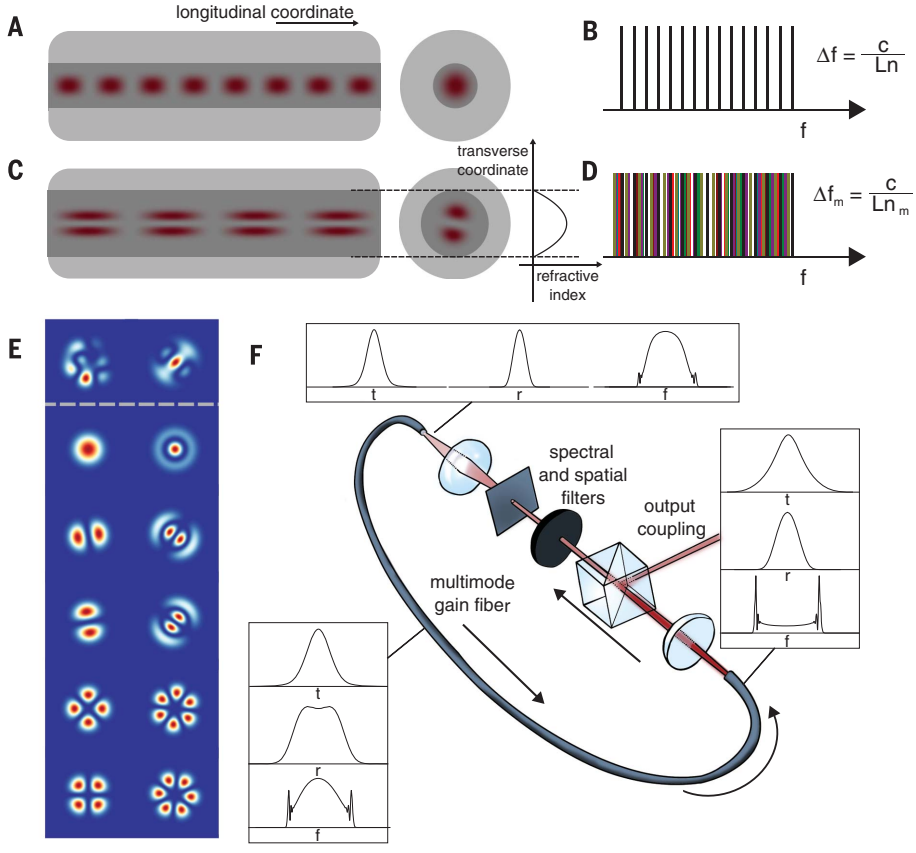

Fig. 1. Conceptual outline of mode-locked multimode fiber lasers. With a single transverse mode, lasing occurs in longitudinal eigenmodes, which correspond to different patterns of the electromagnetic lasing field along the length of the fiber (**A**) and resonant frequencies (**B**). Δf, free spectral range; c, speed of light; L, laser cavity length; n, group index; Δf_m, free spectral range of each transverse mode family m; n_m, group index of transverse mode family m. In a multimode (MM) laser cavity, the lasing eigenmodes describe 3D electromagnetic field patterns. One 3D mode is illustrated in (**C**). In a MM laser cavity, the resonant frequency spectrum (**D**) and transverse field distribution [two examples shown at the top of (E)] can be complicated. A family of longitudinal modes corresponds to each transverse mode [lower part of (E), different colors in (D)]. In a MM fiber, all possible transverse field distributions can be decomposed into contributions from these transverse eigenmodes (**E**). (**F**) Simulated evolution of intensity profiles in a spatiotemporally mode-locked state. t, time; r, transverse spatial coordinate; f, frequency.

longitudinal modes. Without gain interactions and because the output is taken directly after the passive GRIN fiber, the continuous-wave (CW) spatial beam profile also reveals the active transverse lasing modes in the cavity when the laser is mode-locked. Temporal measurements (such as those shown in Fig. 2, F and G; figs. S1 and S2; and movie S1) demonstrate that this spatiotemporal self-organization results in single pulses comprising many nondegenerate transverse mode families, as predicted by our simulations.

For understanding and applications alike, it is important to determine whether STML can still occur when slow transverse gain interactions are present. Informed by results from the first cavity, we investigated spatiotemporal mode-locking in a second cavity based completely on a partially graded, highly MM Yb-doped gain fiber (fig. S17). With necessarily weaker spatial filtering and richer mixture of spatial and spatiotemporal nonlinear interactions, theoretical modelling and analysis of this scenario is more complicated than for the previous cavity. Nonetheless, we developed a qualitative spatiotemporal model that incorporates all relevant effects. This model (supplementary text) shows that the key principals of STML carry over from the simpler cavity. With high power, as well as spectral and spatial filtering, we observe many different complex spatiotemporal dynamics in numerical simulations (figs. S18 to S25), including stable mode-locked pulse trains.

We constructed a corresponding laser similar to the previously described cavity, except all of the fiber is the highly MM, partially GRIN Yb-doped gain fiber (Nufern FUD-7005), and spatial filtering is supplemented by an adjustable slit or iris (Fig. 1F, methods, and fig. S26). Above a threshold pump power, STML lasing states are observed (Fig. 3). As the pump power is adjusted, we observe discontinuous changes in the field's spatial, temporal, and spectral properties as the laser undergoes the transition from CW lasing in 10 to 100 transverse modes to MM mode-locking where the output beam comprises ~2 to 10 modes. As with the previous cavity, this observation provides strong evidence for STML. Further temporal measurements (Fig. 3, D and E) and additional analysis provide strong evidence that the produced pulses comprise multiple transverse mode families (for further details, see materials and methods and supplementary text).

For this cavity, again a wide variety of different mode-locked states are observed for different configurations (fig. S29). However, the minimum power for which mode-locking occurs in this laser corresponds to intracavity powers >100 kW. Consequently, systematic exploration of this laser and future engineering of practical instruments will require application of known techniques for avoiding fiber damage. Furthermore, direct measurements of the 3D field will be an important step for increased understanding of STML. Ongoing developments in this direction are promising (*24*).

Investigation of 3D mode-locking will connect scientifically to areas well beyond short-pulse generation. The dimensionality and controllable dissipation and disorder make consideration of wave turbulence and condensation (*25*, *26*) especially interesting. With longer or suitably designed fibers, disorder can be introduced controllably, thereby bridging the gap to random lasers and allowing exploration of the entire parameter space of MM lasing (*19*, *20*). Although disorder is weak in the present work, recent research indicates that MM self-organization may be robust to disorder (*12*–*16*). This will be important for applications, which will ultimately require environmental stability. In addition, mode-locked lasers are closely related to coherently driven microresonators, where the influence of higher-order transverse modes is starting to be considered (*27*–*29*). Spatiotemporal mode-locking and related phenomena should be possible in these systems and should provide new features for frequency comb applications.

MM mode-locked lasers have considerable potential for high performance. Initial results obtained with the second cavity (150-nJ and 150-fs pulses, for ~1-MW peak power and ~10-W average power) already rival the best achieved with flexible, large-area single-mode fibers (*30*). With larger fiber-core areas, we expect that, in principle, scaling of pulse energy by more than two orders of magnitude will be possible (figs. S20 and S21). At the highest pulse energies, simulations predict the emergence of a stable MM Gaussian output beam, which will be useful for applications (fig. S18).

Exploration of the full scope of MM mode-locking will require developments on several

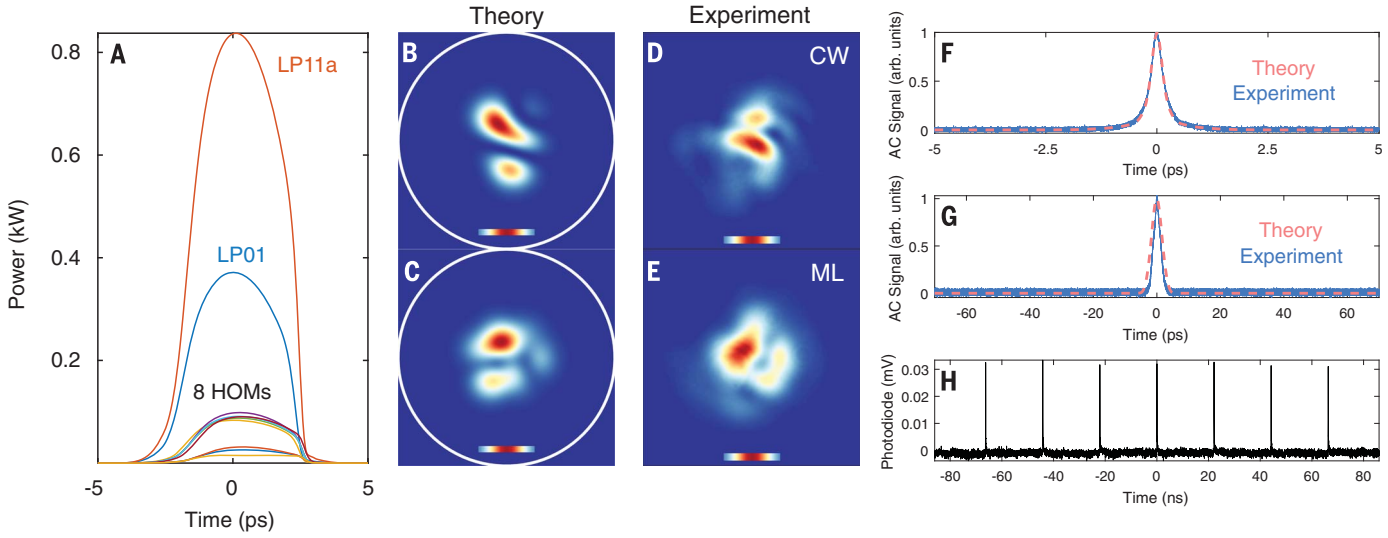

Fig. 2. Characterization of a spatiotemporally mode-locked pulse train: theory and experiment. (**A**) Simulated mode-resolved pulse intensity in 10 transverse modes. HOMs, higher-order modes. (**B** and **C**) Simulated continuous-wave (CW) and mode-locked (ML) near-field beam profiles. (**D** and **E**) Same as in (B) and (C) for the experiment. (**F**) Dechirped intensity autocorrelation for both simulation and experiment. (**G**) Autocorrelation for the chirped pulse over a 140-ps range. (**H**) Pulse train measured using a photodiode with a ~40-ps resolution. The MM beam in (E) corresponds to a single pulse that comprises >10 locked transverse modes, with no CW background. This figure is extended in figs. S1 to S4. Real-time acquisition of the experimental measurements, additional demonstrations, and animations of the numerical results are shown in movie S1. All mode-locked states examined in this manuscript are self-starting.

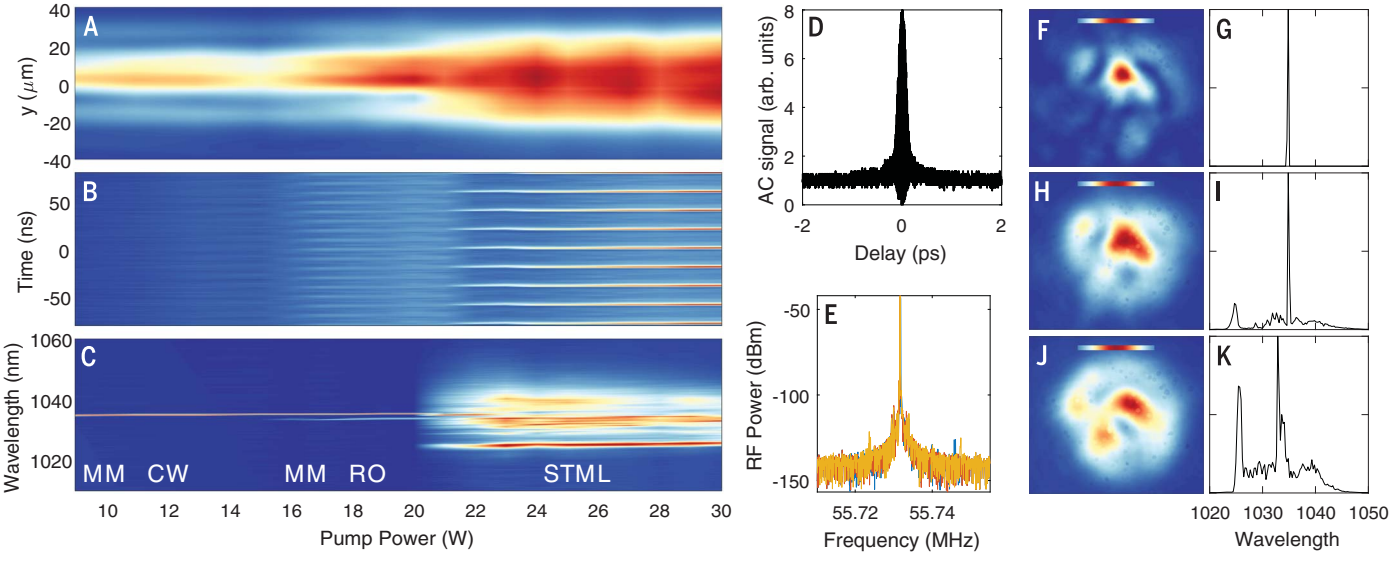

Fig. 3. Transition to mode-locking in the second laser cavity. (**A** to **C**) Variation with pump power of (A) the near-field beam profile integrated over one dimension, (B) the output, and (C) the spectrum. (**D** to **K**) As the pump power is changed, the field transitions from MM continuous-wave lasing (MM CW) [(F) and (G)] to relaxation oscillations (MM RO) then to bistability with relaxation oscillations (~20 to 23 W) [(H) and (I)] and then to STML [(D), (E), (J), and (K)]. The CW lasing threshold is 9 W. The coherence of the mode-locked state is evident from the autocorrelation of the dechirped pulse (D) and the radio frequency (RF) spectra [(E), where the different colors correspond to measurements taken at different arbitrary positions on the beam]. The scale bars in (F), (H), and (J) show the Gaussian profile of the fundamental mode of the fiber. dBm, decibel-milliwatts.

fronts, including measurement capabilities. The ability to generate high-power and spatiotemporally engineered coherent light fields should lead to breakthroughs in laser science, as well as applications.

REFERENCES AND NOTES

1. A. L. Schawlow, C. L. Townes, *Phys. Rev.* **112**, 1940–1949 (1958).
2. S. T. Cundiff, J. Ye, *Rev. Mod. Phys.* **75**, 325–342 (2003).
3. D. Auston, *IEEE J. Quantum Electron.* **4**, 420–422 (1968).
4. P. W. Smith, *Appl. Phys. Lett.* **13**, 235–237 (1968).
5. D. Côté, H. M. van Driel, *Opt. Lett.* **23**, 715–717 (1998).
6. F. Poletti, P. Horak, *J. Opt. Soc. Am. B* **25**, 1645–1654 (2008).
7. H. Pourbeyram, G. P. Agrawal, A. Mafi, *Appl. Phys. Lett.* **102**, 201107 (2013).
8. T. Hellwig, T. Walbaum, C. Fallnich, *Appl. Phys. B* **112**, 499–505 (2013).
9. E. Nazemosadat, A. Mafi, *Opt. Express* **21**, 30739–30745 (2013).

10. J. Demas *et al*., *Optica* **2**, 14–17 (2015).
11. L. G. Wright, W. H. Renninger, D. N. Christodoulides, F. W. Wise, *Opt. Express* **23**, 3492–3506 (2015).
12. K. Krupa *et al*., *Nat. Photonics* **11**, 237–241 (2017).
13. L. G. Wright *et al*., *Nat. Photonics* **10**, 771–776 (2016).
14. Z. Liu, L. G. Wright, D. N. Christodoulides, F. W. Wise, *Opt. Lett.* **41**, 3675–3678 (2016).
15. G. Lopez-Galmiche *et al*., *Opt. Lett.* **41**, 2553–2556 (2016).
16. R. Guenard *et al*., *Opt. Express* **25**, 4783–4792 (2017).
17. D. J. Richardson, J. M. Fini, L. E. Nelson, *Nat. Photonics* **7**, 354–362 (2013).
18. H. Cao *et al*., *Phys. Rev. Lett.* **82**, 2278–2281 (1999).
19. C. Conti, M. Leonetti, A. Fratalocchi, L. Angelani, G. Ruocco, *Phys. Rev. Lett.* **101**, 143901 (2008).
20. F. Antenucci, A. Crisanti, M. Ibáñez-Berganza, A. Marruzzo, L. Leuzzi, *Philos. Mag.* **96**, 704–731 (2016).
21. M. Nixon *et al*., *Nat. Photonics* **7**, 919–924 (2013).
22. W. H. Renninger, A. Chong, F. W. Wise, *IEEE J. Sel. Top. Quantum Electron.* **18**, 389–398 (2012).
23. A. Chong, L. G. Wright, F. W. Wise, *Rep. Prog. Phys.* **78**, 113901 (2015).
24. Z. Guang, M. Rhodes, M. Davis, R. Trebino, *J. Opt. Soc. Am. B* **31**, 2736–2743 (2014).
25. A. Picozzi *et al*., *Phys. Rep.* **542**, 1–132 (2014).
26. E. G. Turitsyna *et al*., *Nat. Photonics* **7**, 783–786 (2013).
27. Y. Liu *et al*., *Optica* **1**, 137–144 (2014).
28. Q.-F. Yang, X. Yi, K. Y. Yang, K. Vahala, *Nat. Phys.* **13**, 53–57 (2016).
29. G. D'Aguanno, C. R. Menyuk, *Phys. Rev. A* **93**, 043820 (2016).
30. M. Baumgartl *et al*., *Opt. Lett.* **35**, 2311–2313 (2010).

ACKNOWLEDGMENTS

L.G.W. performed experiments and simulations. L.G.W. and F.W.W. wrote the first drafts of the manuscript. F.W.W. and D.N.C. provided funding and supervised the project. All authors contributed to the final manuscript. L.G.W. and F.W.W. have submitted a patent application for spatiotemporally mode-locked lasers. This work was supported by Office of Naval Research grant N00014-13-1-0649 and NSF grant ECCS-1609129. We thank Z. Ziegler for discussions and contributions to some of the numerical codes used for MM GNLSE simulations, Z. Liu for discussions and his early contribution to the work, E. Falco for the laser schematic in Fig. 1F, and W. Renninger for his critical review of an early version of the manuscript. All data presented in this Report and the supplementary materials are available on reasonable request to L.G.W.

SUPPLEMENTARY MATERIALS

www.sciencemag.org/content/358/6359/94/suppl/DC1
Materials and Methods
Supplementary Text
Figs. S1 to S33
References (*31*–*35*)
Movie S1

14 June 2017; accepted 30 August 2017
10.1126/science.aao0831

Spatiotemporal mode-locking in multimode fiber lasers

Logan G. Wright, Demetrios N. Christodoulides and Frank W. Wise

Science **358** (6359), 94-97.
DOI: 10.1126/science.aao0831

Harnessing complexity in laser light

The development of lasers and the quality of the output light has been crucially dependent on understanding and being able to control the process occurring within the laser-generating cavity. In a real laser cavity, there are both longitudinal and transverse modes; for the highest-quality lasers, reducing the effects of the latter has been standard practice. However, using a graded index fiber cavity, Wright *et al.* demonstrate that the longitudinal and transverse modes can be locked to provide an output of complex coherent light. Harnessing, rather than filtering out, the transverse modes could produce a valuable and flexible light source applicable across a broad range of disciplines.

Science, this issue p. 94